Correlation Analysis in Time-of-Flight Calibration of BESIII *

HU Ji-Feng[1,2;1)] HE Kang-Lin[2;2)] ZHANG Zi-Ping[1] BIAN Jian-Ming[2,3] CAO Guo-Fu[2,3] DENG Zi-Yan[2]
HE Miao[2,3] HUANG Bin[2,3] JI Xiao-Bin[2] LI Gang[2,4] LI Hai-Bo[2] LI Wei-Dong[2] LIU Chun-Xiu[2]
LIU Huai-Min[2] MA Qiu-Mei[2] MA Xiang[2,3] MAO Ya-Jun[5] MAO Ze-Pu[2] MO Xiao-Hu[2] QIU Jin-Fa[2]
SUN Sheng-Sen[2] SUN Yong-Zhao[2,3] WANG Ji-Ke[2,3] WANG Liang-Liang[2,3] WEN Shuo-Pin[2]
WU Ling-Hui[2,3] XIE Yu-Guang[2,3] YANG Ming[2,3] YOU Zheng-Yun[5] YU Guo-Wei[2]
YUAN Chang-Zheng[2] YUAN Ye[2] ZANG Shi-Lei[2,4] ZHANG Chang-Chun[2]
ZHANG Jian-Yong[2,4] ZHANG Ling[6] ZHANG Xue-Yao[7] ZHANG Yao[7]
ZHENG Zhi-Peng[2] ZHU Yong-Sheng[2] ZOU Jia-Heng[7]

1 (Department of Modern Physics, University of Science and Technology of China, Hefei 230026, China)
2 (Institute of High Energy Physics, CAS, Beijing 100049, China)
3 (Graduate University of Chinese Academy of Sciences, Beijing 100049, China)
4 (CCAST(World Laboratory), Beijing 100080, China)
5 (Peking University, Beijing 100871, China)
6 (Hunan University, Changsha 410082, China)
7 (Shandong University, Ji'nan 250100, China)

Abstract The errors and correlations of BESIII TOF measurements are carefully checked in hit position at z partitions with the electron-pair events. The measured time-of-flight's and their covariance matrices are subjected to a correlation analysis algorithm which is developed for BESIII to combine the independent measurements with common errors. Monte Carlo studies show that the correlated analysis can provide more reliable TOF information on particle identification.

Key words time-of-flight, particle identification, offline calibration, time resolution, errors and correlations

1 Introduction

The BEPC(Beijing Electron Positron Collider) Ⅱ is a double-ring, multi-bunch collider with the designed luminosity approximately 100 times higher than that of BEPC. The Beijing Spectrometer (BES) Ⅲ will operate at BEPC Ⅱ and denote the abundant $\tau-$charm physics. The BESⅢ detector[1, 2] consists of a beryllium beam pipe, a helium-based small-celled drift chamber, Time-of-Flight (TOF) counters for particle identification, a CsI(Tl) crystal calorimeter, a super-conducting solenoidal magnet with a field of 1T, and a muon identifier of Resistive Plate Counters (RPC) interleaved with the magnet yoke plates.

The TOF system is crucial for particle identification (PID). It consists of a two-layer barrel array of 8850mm×60mm×2320mm BC408 scintillators in each layer and one-layer endcap array of 48 fan-shaped BC404 scintillators at each side, the expected time resolution for two layers is from 100 to 110ps for kaons and pions, giving a 2σ K/π separation up to 0.9GeV/c for normal tracks.

Received 31 December 2006
* Supported by CAS Knowledge Innovation Project (U-602, U-34), National Natural Science Foundation of China (10491300, 10605030) and 100 Talents Program of CAS (U-54, U-25)
1) E-mail: hujf@ihep.ac.cn
2) E-mail: hekl@ihep.ac.cn

The PID ability depends on the time resolution of TOF system. There are many factors which affect the TOF measurements[1]. They can be classified into two major categories: the un-correlated parts and the correlated parts. The un-correlated uncertainty is dominated by the detector resolution. The correlated uncertainty of TOF measurements is mainly caused by the beam bunch spread (∼40ps for BESIII), which must be taken into account. In this paper, we present a correlation analysis in TOF calibration/reconstruction software system[3] for BESIII.

2 The calibration of TOF measurement in each readout unit

Electrons from 5×10^4 generated Bhabha events are used for calibration. The $e^+e^-\to(\gamma's)e^+e^-$ data are produced with BHLUMI[4] generator, and subjected to a Geant4[5] based detector simulation program BOOST[6], in which the generation and transport of optical photons in TOF counter are taken into account. The simulated data are processed in the BES Offline Software System (BOSS)[7].

2.1 The time-of-flight calibration

The calibration of TOF is proceeded by comparing the measured time $t_{\rm mea}=t_{\rm raw}-t_0-t_{\rm cor}$ against the predicted time $t_{\rm exp}=L/\beta c$, where $t_{\rm raw}$ is the TDC value recorded by electronics, t_0 the event start time, $t_{\rm cor}$ the correction term; c is the velocity of light in vacuum, $\beta=p/\sqrt{p^2+m^2}$, the flight velocity of charged particle, m the particle mass, L and p are the corresponding flight path and momentum measured by the MDC(Main Drift Chamber). The correction term ($t_{\rm cor}$) is a function of pulse height Q and hit position z, we take the following empirical form[8]

$$t_{\rm cor}=P_0+\frac{P_1+P_2\cdot z+P_3\cdot z^2}{\sqrt{Q}}+P_4\cdot Q+P_5\cdot Q^2+P_6\cdot Q^3+P_7\cdot z+P_8\cdot z^2+P_9\cdot z^3+\frac{P_{10}}{R^2+z^2}+t_0^{\rm offset}, \quad (1)$$

where R is the inner radius of TOF detector, $P_i(i=0,1,\cdots,10)$ are the calibration constants. In Eq. (1), the P_0 represents the delay time, such as cabling, etc.; the correction function of time walk effect is represented by the terms containing P_1 to P_3, then a polynomial containing P_4 to P_6 is used to describe the saturation of PMTs, etc.; while the polynomial containing P_7 to P_9 describes the correction to the effective velocity of light in the scintillator; the term with P_{10} is used to correct the effect caused by different depths of charged track traversing in scintillator. The $t_0^{\rm offset}$ is an additional term to correct the t_0 offsets run-by-run, which is set to be zero at present.

A χ^2 minimization method is applied by defining a set of

$$\chi^2({\rm counter,readout\ unit})=\sum^{\rm events}(t_{\rm mea}-t_{\rm exp})^2, \quad (2)$$

in each readout unit and counter-by-counter. The calibration constants, P_0 to P_{10}, are obtained from data by setting the derivative of Eq. (2) with respect to P_i to zero.

As shown in Fig. 1, the time resolution is improved from ∼251ps to ∼118ps. For the calibration of endcap counters, the expression of $t_{\rm cor}$ is similar to that of Eq. (1), only the variable z is replaced by r, the hit position in radial direction.

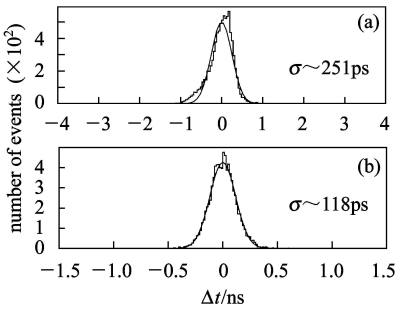

Fig. 1. $\Delta t=t_{\rm mea}-t_{\rm exp}$ distributions: (a) before and (b) after calibration for one-end of readout unit of barrel TOF counter.

2.2 The pulse height (Q) calibration

The ionization of a charged particle generates optical photons while traversing the TOF counter. The resulting photoelectron signal depends on the collection and transport efficiency of the optical package and the quantum efficiency of the PMT. Plastic scintillators do not respond linearly to the ionization density. A widely used semi-empirical formula by Birks is[9]

$$\frac{{\rm d}L}{{\rm d}x}=L_0\frac{{\rm d}E/{\rm d}x}{1+\kappa_{\rm B}{\rm d}E/{\rm d}x}\ , \quad (3)$$

where L is the luminescence, L_0 the luminescence at low specific ionization density ($\mathrm{d}E/\mathrm{d}x$), and κ_B the Birks' constant, which must be determined for each scintillator by measurements[10].

The pulse height Q_i (raw ADC) at each readout PMT can be written as:

$$\begin{aligned} Q_1 &= A_1 \times \frac{Q_0}{\sin\theta} \times \exp\left(-\frac{l/2+z}{L_\mathrm{atten}}\right), \\ Q_2 &= A_2 \times \frac{Q_0}{\sin\theta} \times \exp\left(-\frac{l/2-z}{L_\mathrm{atten}}\right), \end{aligned} \tag{4}$$

where l is the total length of scintillator, z the hit position in scintillator, L_atten the transmission attenuation of scintillator, θ the incident angle of charged track, Q_0 the normalized pulse height at $z=0$ and $\theta=90^\circ$, $A_i(i=1,2)$ the amplification coefficient of PMT. From Eq. (4), we get

$$\log\left(\frac{Q_1}{Q_2}\right) = \log\left(\frac{A_1}{A_2}\right) - \frac{2z}{L_\mathrm{atten}} \ . \tag{5}$$

L_atten and A_1/A_2 can be easily determined from the calibration data. Thus Q_0 could be expressed as

$$Q_0 = \frac{\sin\theta}{A_2} \times \frac{Q_1 \exp\left(\frac{l/2+z}{L_\mathrm{atten}}\right) + Q_2 \exp\left(\frac{l/2-z}{L_\mathrm{atten}}\right)}{1+A_1/A_2}. \tag{6}$$

Using μ-pair events, $A_i(i=1,2)$ could be adjusted and normalized counter-by-counter. Here, Q_0's are supposed to be normalized. As shown in Fig. 2(a), the distribution of Q_0 is skewed toward high value (Landau tail). Like the $\mathrm{d}E/\mathrm{d}x$ curve, the variation of Q_peak with $\beta\gamma$ can be calibrated with the hadron, cosmic ray and radiative Bhabha events to an empirical formula

$$Q_\mathrm{peak} = \frac{P_1}{\beta^{P_4}} \left\{ P_2 - \beta^{P_4} - \log\left[P_3 + \left(\frac{1}{\beta\gamma}\right)^{P_5} \right] \right\}, \tag{7}$$

where Q_peak is the maximum probability value of Q_0, $\beta\gamma = p/m$, p and m the corresponded momentum and mass of charged track, $\beta = p/\sqrt{p^2+m^2}$; the parameter $P_i(i=1,5)$ are determined from data. The Q_peak-curve is drawn in Fig. 2(b), which could be applied in particle identification with TOF-Q[11] and the time-of-flight offset correction for hadrons[12].

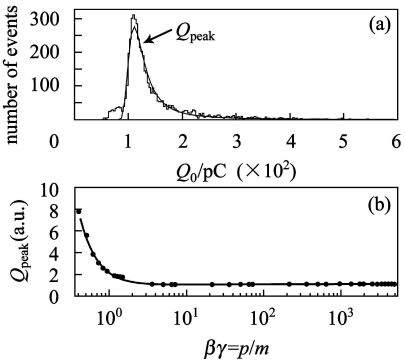

Fig. 2. (a) Q_0 distribution for electrons (p=1.5GeV), the histogram is fitted by a Landau function. (b) Q_peak varies with $\beta\gamma(=p/m)$, the Q_peak-curve is fitted with the function described by Eq. (7). In (a), the concentration of Q_0 below 100pC is mainly caused by the hits at the edge of scintillator.

3 The correlated analysis in TOF calibration

When one charged particle passes through the barrel array of scintillators, it will produce signals in one or two layers of TOF counter, corresponding to two or four measurements for time-of-flight. However, at BESIII the problem of averaging more than one TOF measurement becomes complicated since the distinctive measurements correlate due to the common event start time. A better choice would be the weighted average of the different measurements.

3.1 General algorithm

Suppose we have n measurements t_i of a particular time-of-flight. Since the measurements are correlated we need more information than just the individual errors. Accordingly, let's define the covariance matrix V_t, whose terms are given by $(V_t)_{ij} = \langle \delta t_i \delta t_j \rangle$, where $\delta t_i = t_i - \overline{t}$, $\overline{t}$ is the average of t_i. The best linear estimator for the TOF which accounts for all measurements, including errors and correlations can be constructed generally as

$$\overline{t} = \sum_i w_i t_i, \qquad \sum_i w_i = 1 \ , \tag{8}$$

where the weights w_i must be found. Writing $\delta\overline{t} = \sum_i w_i \delta t_i$ and using the definition of the standard de-

viation, we get

$$\sigma_{\bar{t}}^2 = \sum_{ij} w_i w_j (V_t)_{ij} \ . \tag{9}$$

To minimize $\sigma_{\bar{t}}^2$ subject to the condition $\sum_i w_i = 1$, we use the Lagrange multiplier technique. Let's write

$$\sigma_{\bar{t}}^2 = \sum_{ij} w_i w_j (V_t)_{ij} + \lambda(\sum_i w_i - 1) \ , \tag{10}$$

and set the derivative of Eq. (10) with respect to the w_i and Lagrange multiplier λ to zero. This give the solution

$$w_i = \frac{\sum_k (V_t^{-1})_{ik}}{\sum_{jk} (V_t^{-1})_{jk}} \ . \tag{11}$$

3.2 Errors and correlations of TOF measurements

The time resolution of TOF (σ_t) can be factorized by a production of $\sigma_t(Q)\cdot\sigma_t(z)$, in which $\sigma_t(Q)$ and $\sigma_t(z)$ are functions of the pulse height Q and the hit position z[12]. The variation of $\sigma_t(Q)$ is complicated, which needs the detailed study on the real data. In this paper, only the z dependent time resolution is taken into account, since the $\sigma_t(z)$'s are in similar manners for electrons, muons and hadrons[12]. Fig. 3 shows a typical variation of $\sigma_t(z)$ in one readout unit as a function of z from the Bhabha event. The time resolution becomes worse while the hit position is far from the readout end.

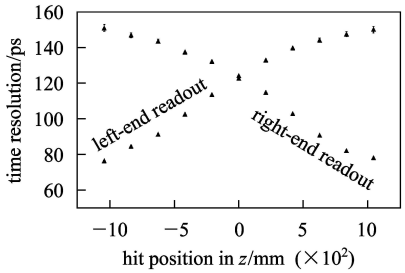

Fig. 3. The variation of $\sigma_t(z)$ for the left-end and the right-end readout unit in barrel TOF counter.

The $t_{\rm mea}$ is obtained by calculating the difference between the end-time and the start-time. The accuracy of end-time is limited by the detector resolution; the precision of start-time is controlled by the uncertainties of t_0. Thus for a given barrel TOF counter, the $t_{\rm mea}$ in the left-end and the right-end readout units can be decomposed as

$$t_1 = t_{\rm c} + (t_{\rm D})_1, \quad t_2 = t_{\rm c} + (t_{\rm D})_2 \ , \tag{12}$$

where t_1 and t_2 represent the $t_{\rm mea}$'s in two readout PMTs, $t_{\rm c}$ represents the common part of time between t_1 and t_2, $(t_{\rm D})_1$ and $(t_{\rm D})_2$ represent the uncorrelated part of t_1 and t_2. The covariance matrix for t_1 and t_2 can be expressed as

$$V_t = \begin{pmatrix} \sigma_1^2 & \sigma_{\rm c}^2 \\ \sigma_{\rm c}^2 & \sigma_2^2 \end{pmatrix}, \tag{13}$$

where σ_1 and σ_2 are the time resolution in the left-end and the right-end readout units, $\sigma_{\rm c}$ the fluctuation of $t_{\rm c}$. According to the definition of covariance matrix, we have the following expressions

$$\begin{aligned} \sigma_1^2 &= \langle \delta t_1 \delta t_1 \rangle = \langle \delta t_{\rm c} \delta t_{\rm c} \rangle + \langle \delta (t_{\rm D})_1 \delta (t_{\rm D})_1 \rangle, \\ \sigma_2^2 &= \langle \delta t_2 \delta t_2 \rangle = \langle \delta t_{\rm c} \delta t_{\rm c} \rangle + \langle \delta (t_{\rm D})_2 \delta (t_{\rm D})_2 \rangle, \\ \sigma_c^2 &= \langle \delta t_1 \delta t_2 \rangle = \langle \delta t_{\rm c} \delta t_{\rm c} \rangle, \end{aligned} \tag{14}$$

by the fact that the correlations $\langle \delta t_{\rm c} \delta (t_{\rm D})_1 \rangle = 0$, $\langle \delta t_{\rm c} \delta (t_{\rm D})_2 \rangle = 0$ and $\langle \delta (t_{\rm D})_1 \delta (t_{\rm D})_2 \rangle \approx 0$.

To get the $\sigma_{\rm c}$ conveniently, let's define two new time variables

$$t_+ = \frac{t_1 + t_2}{2}, \quad t_- = \frac{t_1 - t_2}{2} \ . \tag{15}$$

The fluctuations of t_+ and t_- can be expressed as

$$\begin{aligned} \sigma_+^2 &= \langle \delta t_+ \delta t_+ \rangle = \frac{\sigma_1^2 + \sigma_2^2}{4} + \frac{\sigma_{\rm c}^2}{2}, \\ \sigma_-^2 &= \langle \delta t_- \delta t_- \rangle = \frac{\sigma_1^2 + \sigma_2^2}{4} - \frac{\sigma_{\rm c}^2}{2}, \end{aligned} \tag{16}$$

where σ_+ and σ_- are the time resolution of t_+ and t_-. The $\sigma_{\rm c}$ can be directly extracted by the calculation of $\sigma_{\rm c} = \sqrt{\sigma_+^2 - \sigma_-^2}$. Fig. 4 shows the distribution of

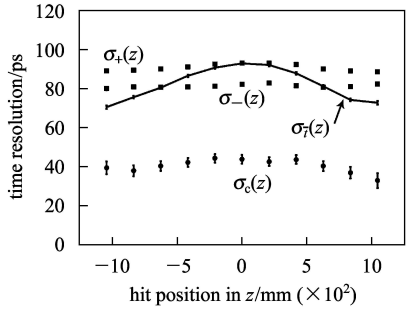

Fig. 4. Time resolution of t_+, t_-, $t_{\rm c}$ and the weighted time $\bar{t}$ for one-layer of TOF measurement.

$\sigma_+(z)$, $\sigma_-(z)$ and $\sigma_c(z)$, where $\sigma_c(z)$ is approximately a constant, around 40ps. Substituting the special expression of Eq. (13) into Eqs. (8)—(11), we get

$$w_1=\frac{\sigma_2^2-\sigma_c^2}{\sigma_1^2+\sigma_2^2-2\sigma_c^2},\quad w_2=\frac{\sigma_1^2-\sigma_c^2}{\sigma_1^2+\sigma_2^2-2\sigma_c^2}, \tag{17}$$

and

$$\sigma_{\bar{t}}^2=\frac{\sigma_1^2\cdot\sigma_2^2-\sigma_c^4}{\sigma_1^2+\sigma_2^2-2\sigma_c^2}\ . \tag{18}$$

The resulting $\sigma_{\bar{t}}$ is drawn in Fig. 4. The average time resolution for one-layer is about 86ps.

3.3 Combining the time-of-flight from two-layer measurements

With the Bhabha events, we found that the correlation term σ_c's in two layer measurements are the same value ($\sim$ 40ps). The weighted time-of-flight and its error in each layer, t_{L_i} and $\sigma_{L_i}(i=1,2)$, can be determined from Eqs. (8), (17) and (18). Similar to the method adopted for one-layer measurement, we can construct the covariance matrix for two-layer measurements as follows

$$V_t=\begin{pmatrix}\sigma_{L_1}^2 & \sigma_{L_c}^2\\ \sigma_{L_c}^2 & \sigma_{L_2}^2\end{pmatrix}, \tag{19}$$

where σ_{L_c} is the correlation between two-layer measurements.

Substituting t_1, t_2 with t_{L1}, t_{L2} in Eqs. (12) and (15), we can get the corresponding errors and correlations. The calculations of the σ_+, σ_- and σ_{L_c} are illustrated in Fig. 5. The correlation between two-layer measurements is almost a constant, $\sim$ 40ps. It agrees fairly well with the results from the two-end measurements in each layer. Thus, we have $\sigma_{L_c}=\sigma_c$.

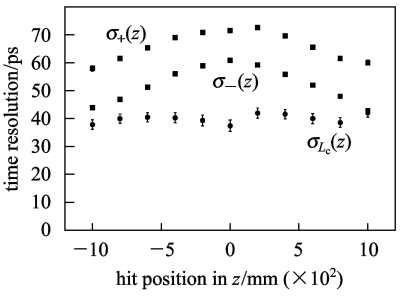

Fig. 5. The correlations between two layer TOF measurements, where $\sigma_{L_c}(z)=\sqrt{\sigma_+^2(z)-\sigma_-^2(z)}$.

The weighted time-of-flight of two-layer measurements can be easily obtained by applying the covariance matrix of Eq. (19) in Eq. (17). The resulting $t_{\rm mea}-t_{\rm exp}$ are drawn in Fig. 6(a). The average time resolution from two-layer measurements is about 68ps, a little bit worse than $86/\sqrt{2}\approx 61$ps, where the value of 86ps is the average time resolution of one-layer measurement.

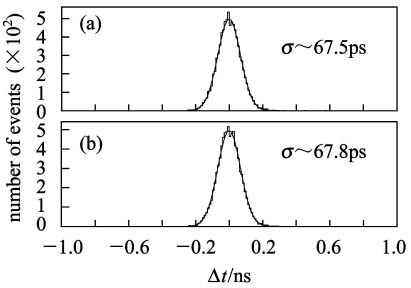

Fig. 6. $\Delta t=t_{\rm mea}-t_{\rm exp}$ distribution: (a) $\bar{t}$ is weighted by $\bar{t}_{L_i}(i=1,2)$, $\bar{t}_{L_i}$'s are the average time in each layer which is weighted by $t_{E_i}(i=1,2)$, t_{E_i}'s are the TOF measurements in each end of readout units; (b) $\bar{t}$ is directly weighted by $t_{E_i}(i=1,2,\cdots,4)$, t_{E_i}'s are the TOF measurements in the four-end of readout units.

The apparatus of barrel TOF array can be treated in such a way that the four independent readout PMTs can measure the time-of-flight for a charged particle. The covariance matrix of TOF measurements can be constructed as

$$V_t=\begin{pmatrix}\sigma_1^2 & \sigma_c^2 & \sigma_c^2 & \sigma_c^2\\ \sigma_c^2 & \sigma_2^2 & \sigma_c^2 & \sigma_c^2\\ \sigma_c^2 & \sigma_c^2 & \sigma_3^2 & \sigma_c^2\\ \sigma_c^2 & \sigma_c^2 & \sigma_c^2 & \sigma_4^2\end{pmatrix}. \tag{20}$$

In Eq. (20), $\sigma_i(i=1,2,\cdots,4)$ are the resolution of all readout units, the correlations (σ_c) between different measurements are taken as the same value ($\sim$ 40ps) by the fact that $c_{\rm EE}=c_{\rm LL}$, where $c_{\rm EE}$'s are the correlation between the two-end of readout units in each layer, $c_{\rm LL}$ is the correlation between two-layer measurements. Employing the covariance matrix Eq. (20) in Eqs. (8)—(11), the weight factors $w_i(i=1,2,\cdots,4)$ can be easily calculated. The resulting $t_{\rm mea}-t_{\rm exp}$ distribution is drawn in Fig. 6(b).

As shown in Fig. 6(a) and 6(b), the resulting time resolutions from two weighted methods are consistent. The standard weighted method adopted in TOF calibration/reconstruction software system of BESIII

will be in two steps: combining the two-end TOF measurements in each layer; calculating the weighted time from the two-layer measurements.

3.4 Run-by-run t_0 offsets correction

The calibration needs a large data sample during detector running. Several data runs will be combined to provide a calibration sample. The t_0 often varies in a period of particular data taking, it must be taken into account[8] in TOF calibration. To get the t_0 offsets correctly, the data samples are grouped run-by-run after the calibration of each readout unit, then subjected to an algorithm developed in Ref. [13] to extract the t_0 event-by-event precisely. The average value of t_0 in each run will return back to Eq. (1) as an additional correction term $t_0^{\rm offset}$.

4 Summary

The reliable particle identification requires the properly combination of two-layer TOF measurements, especially in the apparatus of BESIII barrel TOF array where the correlations (∼40ps) between TOF measurements in each readout unit are sizable compared with the intrinsic time resolution of the detector(∼110ps per readout unit).

The errors and correlations of TOF measurements are investigated with the simulated electron-pair events in calibration. The elements of resulting covariance matrix are consistent well with the input parameters in the detector simulation. The Monte Carlo studies show that the common errors due to the uncertainty of t_0 can be properly extracted from electron-pair events in one particular run. With the time resolution function $\sigma_{\rm t}(Q,z)$ obtained from the desired samples, the covariance matrix for hadrons can be easily constructed. Thus, we can apply the correlation analysis for hadrons in TOF particle identification.

The authors gratefully acknowledge Dr. JIANG Lin-Li for his contributions to the TOF reconstruction software.

References

1 BESIII Design Report. Interior Document in Institute of High Energy Physics, 2004
2 Harris F A (BES Collab.). arXiv:physics/0606059
3 JIANG Lin-Li. P.H.D Thesis, University of Sciences and Technology, 2006 (in Chinese)
(蒋林立. 中国科学技术大学博士论文, 2006)
4 Jadach S et al. Comput. Phys. Commun., 1992, **70**: 305
5 Agostinelli S et al (Geant4 Collab.). Nucl. Instrum. Methods, 2003, **A506**: 250
6 DENG Zi-Yan et al. HEP & NP, 2006, **30(5)**: 371—377 (in Chinese)
(邓子艳等. 高能物理与核物理, 2006, **30**(5): 371—377)
7 LI Wei-Dong, LIU Huai-Min et al. The Offline Software for the BESIII Experiment. Proceeding of CHEP06. Mumbai, India, 2006
8 RONG Gang et al. HEP & NP, 2001, **25**: 154 (in Chinese)
(荣刚等. 高能物理与核物理, 2001, **25**: 154)
9 Birks J B. Proc. Phys. Soc., 1951, **A64**:295
10 Craun R L, Smith D L. Nucl. Instrum. Methods, 1970, **80**: 239—244
11 LIU Fang, HE Kang-Lin et al. HEP & NP, 2005, **29(8)**: 781—786 (in Chinese)
(刘芳, 何康林等. 高能物理与核物理, 2005, **29**(8): 781—786)
12 SUN Sheng-Sen, HE Kang-Lin et al. HEP & NP, 2005, **29**(2): 162—167 (in Chinese)
(孙胜森, 何康林等. 高能物理与核物理, 2005, **29**(2): 162—167)
13 SUN Yong-Zhao, HE Kang-Lin et al. HEP & NP, 2007, **31**(5): 423 (in Chinese)
(孙永昭, 何康林等. 高能物理与核物理, 2007, **31**(5): 423)

北京谱仪Ⅲ飞行时间计数器系统刻度中的关联分析*

胡继峰[1,2;1)]　何康林[2;2)]　张子平[1]　边渐鸣[2,3]　曹国富[2,3]　邓子艳[2]　何苗[2,3]　黄彬[2,3]
季晓斌[2]　李刚[2,4]　李海波[2]　李卫东[2]　刘春秀[2]　刘怀民[2]　马秋梅[2]　马想[2,3]
冒亚军[5]　毛泽普[2]　莫晓虎[2]　邱进发[2]　孙胜森[2]　孙永昭[2,3]　王纪科[2,3]
王亮亮[2,3]　文硕频[2]　伍灵慧[2,3]　谢宇广[2,3]　杨明[2,3]　尤郑昀[5]　俞国威[2]
苑长征[2]　袁野[2]　臧石磊[2,4]　张长春[2]　张建勇[2,4]　张令[6]
张学尧[7]　张瑶[7]　郑志鹏[2]　朱永生[2]　邹佳恒[7]

1 (中国科学技术大学近代物理系　合肥　230026)
2 (中国科学院高能物理研究所　北京　100049)
3 (中国科学院研究生院　北京　100049)
4 (中国高等科技中心　北京　100080)
5 (北京大学　北京　100871)
6 (湖南大学　长沙　410082)
7 (山东大学　济南　250100)

摘要　利用电子对事例对北京谱仪Ⅲ飞行时间的测量误差, 以及不同测量之间的关联因子随击中位置的变化进行了仔细的研究. 加权的飞行时间由不同的测量值及其相关的误差矩阵计算而得. 蒙特卡罗研究表明. 为北京谱仪Ⅲ开发的关联分析算法可以正确地处理包含公有误差项的多个实验测量结果的合并, 并且能够为粒子鉴别提供可靠的飞行时间信息.

关键词　飞行时间　粒子鉴别　离线刻度　时间分辨　误差及其关联

2006 – 12 – 31 收稿
* 中国科学院知识创新工程(U-602, U-34), 国家自然科学基金(10491300, 10605030)和中国科学院百人计划(U-54, U-25)资助
1) E-mail: hujf@ihep.ac.cn
2) E-mail: hekl@ihep.ac.cn